Recent Results on proton-CT

Prima – RDH – IRPT Collaboration

C. Civinini[1], M. Bruzzi[1,2], M. Intravaia[1,3], N. Randazzo[4], M. Rovituso[5], M. Scaringella[1], V. Sipala[6,7], F. Tommasino[5,8]

[1]INFN - Florence, Florence, Italy
[2]Physics and Astronomy Department, University of Florence, Florence, Italy
[3]Information Engineering and Mathematical Sciences Department, University of Siena, Italy
[4]INFN - Catania, Catania, Italy
[5]INFN - TIFPA, Trento, Italy
[6]INFN - Laboratori Nazionali del Sud, Catania, Italy
[7]Chemistry and Pharmacy Department, University of Sassari, Sassari, Italy
[8]Physics Department, University of Trento, Trento, Italy

Interdisciplinary aspects and applications related to the SPES project
Ferrara, January 29th - 30th 2019

SPES exotic beams for science

Why proton Computed Tomography?

Hadron therapy exploits the sharp shape of the Bragg peak to precisely irradiate a tumor.
But to define an effective treatment plan to potentially reduce inaccuracies in tumor irradiation we need:

Direct measurement of the 3D proton relative (to water) stopping power maps (RSP).

Treatment planning presently uses proton stopping power maps extracted from x-ray CTs resulting in errors on Bragg peak position up to *a few millimeters*.

B. Schaffner and E. Pedroni Phys. Med. Biol. ***43 (1998) 1579–1592***

Hounsfield Units Vs Relative stopping Power

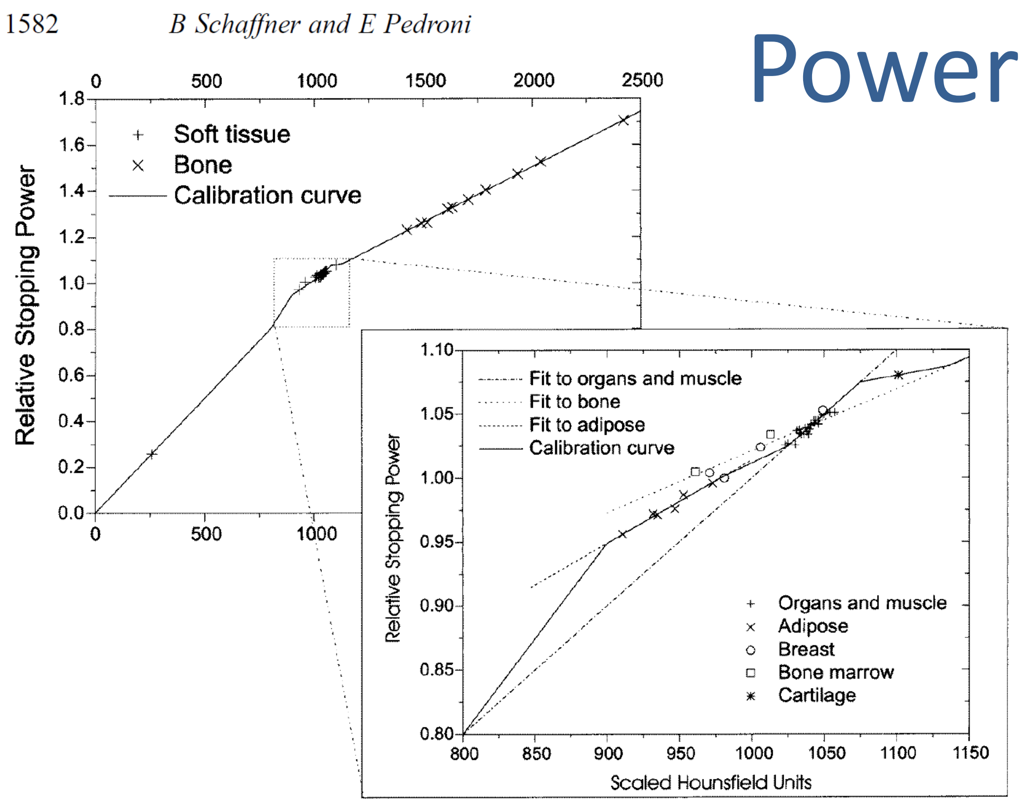

The proton range error due to the HU/RSP conversion depends on the tumor depth and the tissues crossed by the beam and could be as large as ~3 mm.

If protons are used to directly determine the RSP maps this error contribution could be eliminated.

B. Schaffner and E. Pedroni Phys. Med. Biol. ***43 (1998) 1579–1592***

Table 1. Two typical proton treatment cases and expected range errors. The expected error in the position of the distal fall-off of the dose distribution is expected to be a few millimetres in typical cases of proton therapy.

	Soft tissue			Bone			Total
	Amount (cm)	wer[a] (cm)	Abs. error (cm)	Amount (cm)	wer[a] (cm)	Abs. error (cm)	Abs. error (cm)
Brain	10	10.3	0.11	1	1.8	0.03	0.14
Prostate (lateral beam)	15	15.5	0.17	5	9	0.16	0.33

[a] Water equivalent range.

How to perform a proton Tomography

To mitigate the effect of the multiple Coulomb scattering we need an ***event-by-event*** measurement:

1) **Tracker** to measure the proton Most Likely Path (MLP) → Silicon microstrip detectors (~70 μm point resolution);

2) **Calorimeter** to assign an energy loss to each proton track → YAG:Ce scintillating calorimeter (~1% energy resolution @ 200 MeV);

3) **Image reconstruction** → Most Likely Path + Algebraic algorithms running on GPUs.

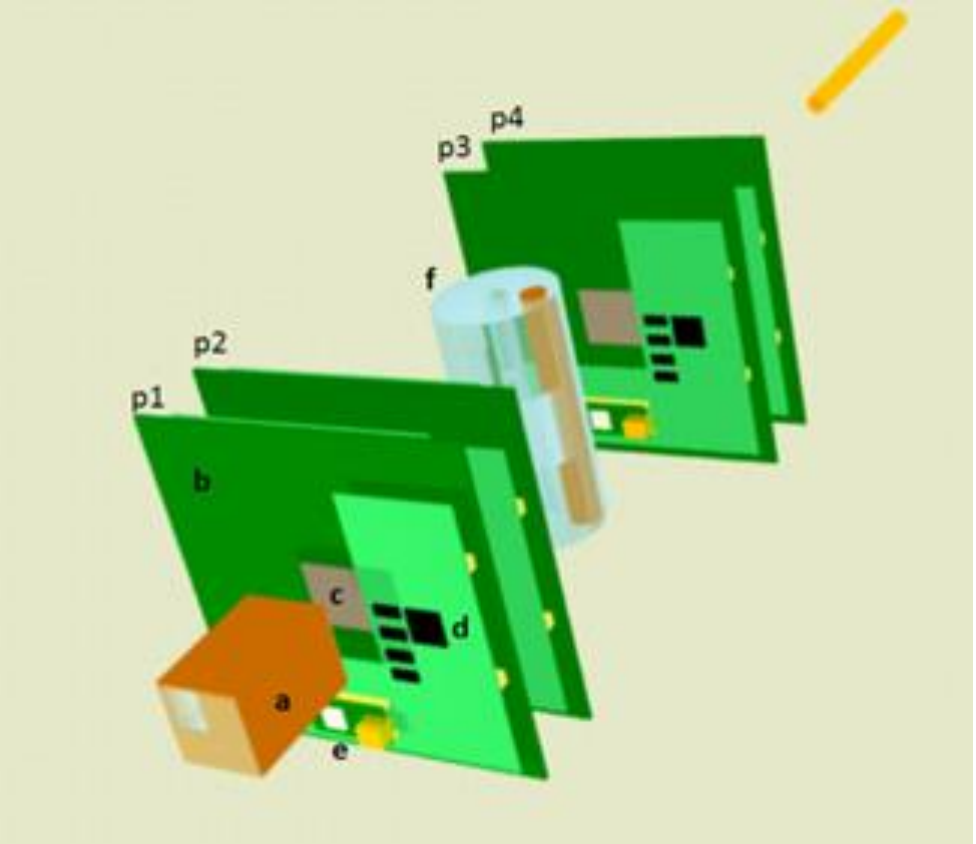

Use a proton beam which is able to cross the patient's body: the residual proton energy (or range) carries information about the stopping power distribution of the traversed material.

Tracking with multiple scattering

Measurements: entry and exit positions and angles

Proton true trajectory

Measurements:
entry position and angle

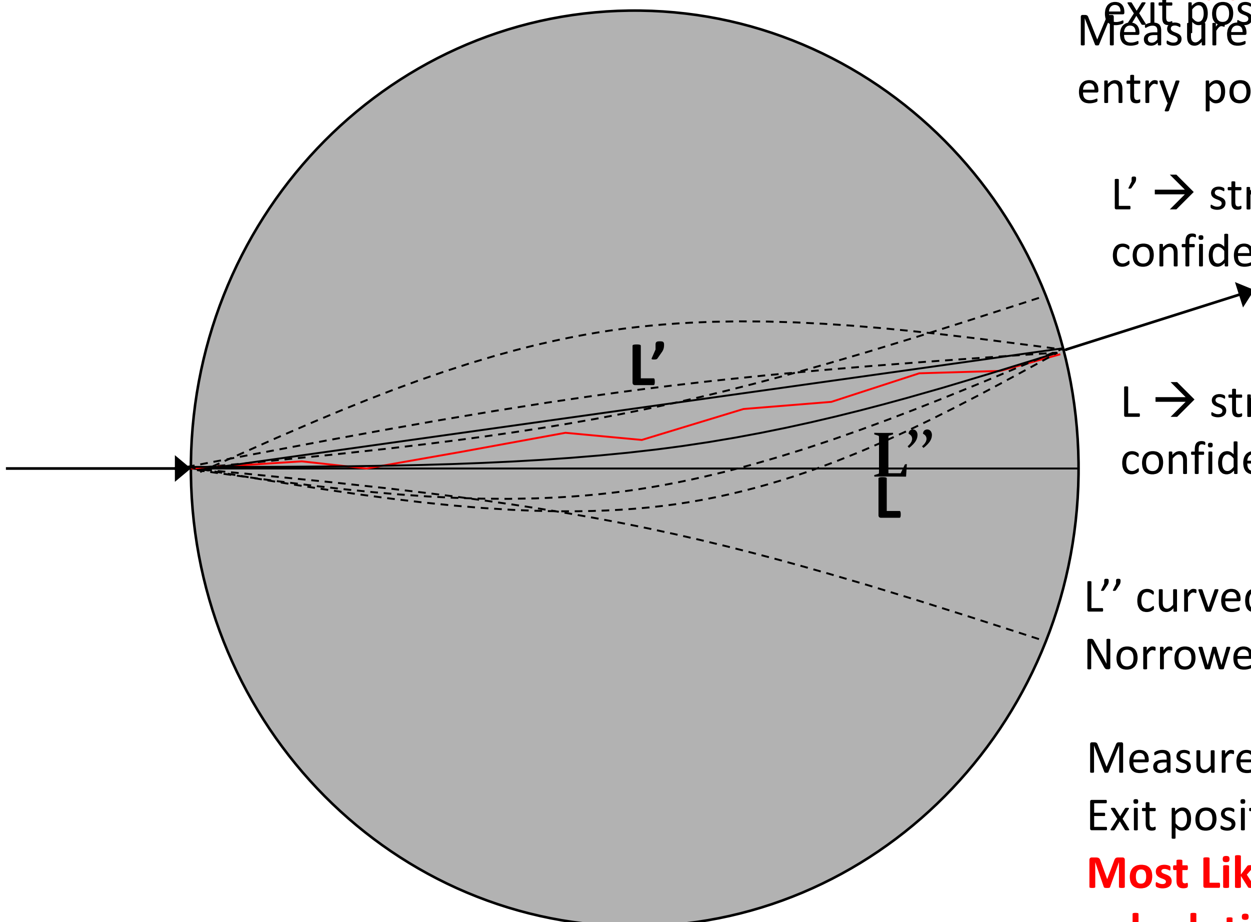

L’ → straight line with confidence limits

L → straight line with confidence limits

L’’ curved trajectory with Norrower confidence limits

Measurements: entry and Exit position and angle + **Most Likely Path (MLP) calculation**

Most Likely Path in a pCT geometry

Starting from D.C. Williams Phys. Med. Biol. **49** (2004) and R.W. Shulte *at al.* Med. Phys. **35 (11)** (2008)
5 cm of air have been inserted in front and behind the 20cm H_2O phantom

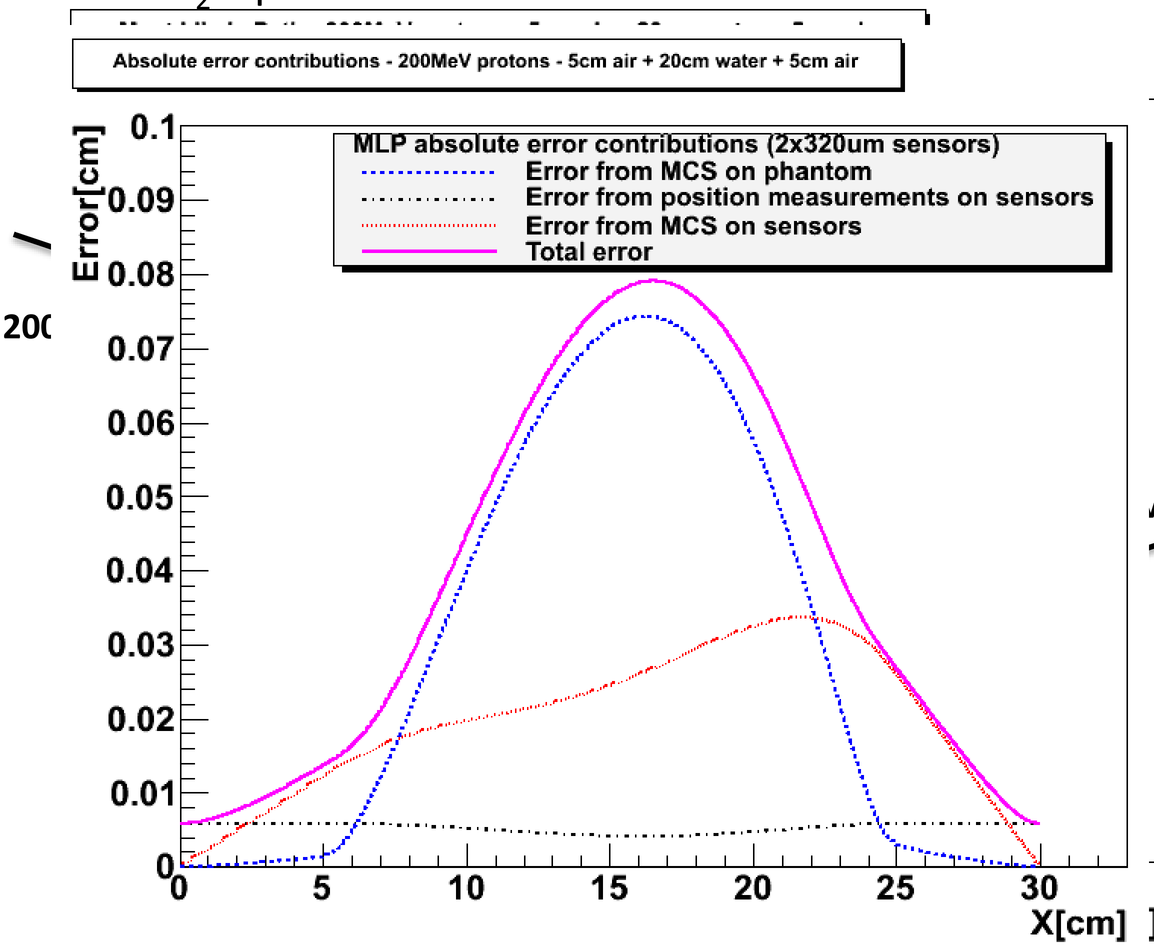

MLP example with 200MeV kinetic energy protons in 20cm of water:

Entry: Y(0) = 0.2cm

Y'(0) = -10mrad

Exit: Y(20) = -0.1cm

Y'(20) = +10mrad

Silicon microstrip detectors:

320μm thick

200μm strip pitch

MLP error envelope plus contributions from detector position measurement error (~ pitch/√12) and MCS inside the silicon sensors →

The sensor thickness contribution affects only the MLP error at the edge of the phantom

σ ~ 150-250μm

Algebraic Reconstruction Techniques

- The tomographic reconstruction problem is to solve, for S_j (stopping power value in pixel *j*), the following set of linear equations:

$$\begin{cases} w_{11}S_1 + w_{12}S_2 + \ \dots + w_{1N}S_N = p_1 \\ w_{21}S_1 + w_{22}S_2 + \ \dots + w_{2N}S_N = p_2 \\ \dots \\ w_{M1}S_1 + w_{M2}S_2 + \ \dots + w_{MN}S_N = p_M \end{cases}$$

- Where:
- $p_i \equiv -\int_{E_{in}}^{E_{out}} [\frac{S}{\rho}(H_2O)]_E^{E_0} dE \quad i = 1, \dots, M; \ w_{ij} = length\ of\ proton\ \boldsymbol{i}\ in\ pixel\ \boldsymbol{j}$
- *N* = number of pixels (unknowns); *M* number of protons (equations)
- $[\frac{S}{\rho}(H_2O)]_E^{E_0}$ proton stopping power in water (norm. to E_0)
- In our case (M>N → the system is over-constrained):
  - *N* = (512x512x64)=16777216 voxels
  - *M* ~ 4-5*10^7 events (in 400 angles)

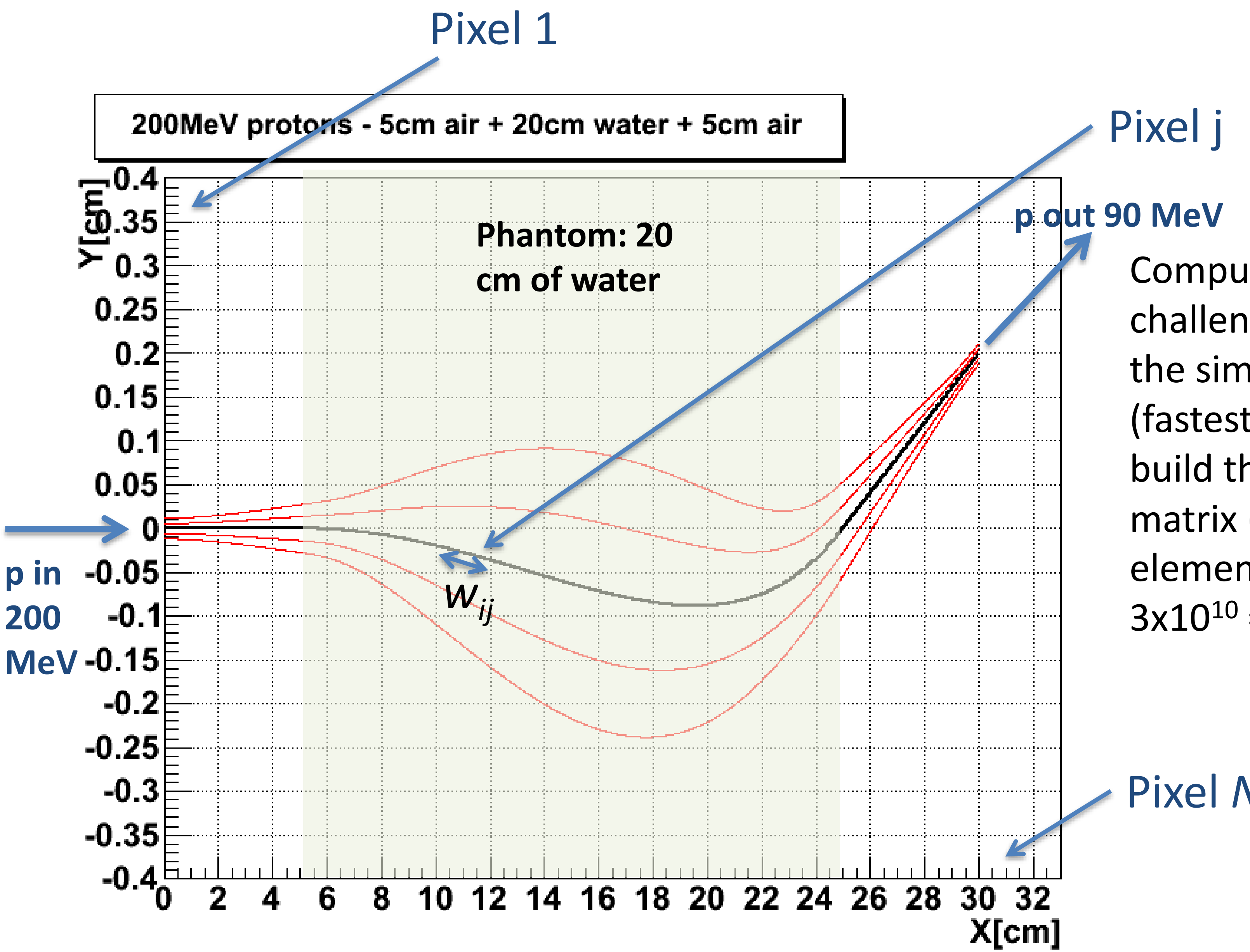

Computational challenge: find the simplest (fastest) way to build the w_{ij} matrix (~10^{15} elements, only $3x10^{10} \neq 0$)

Algebraic Reconstruction Techniques

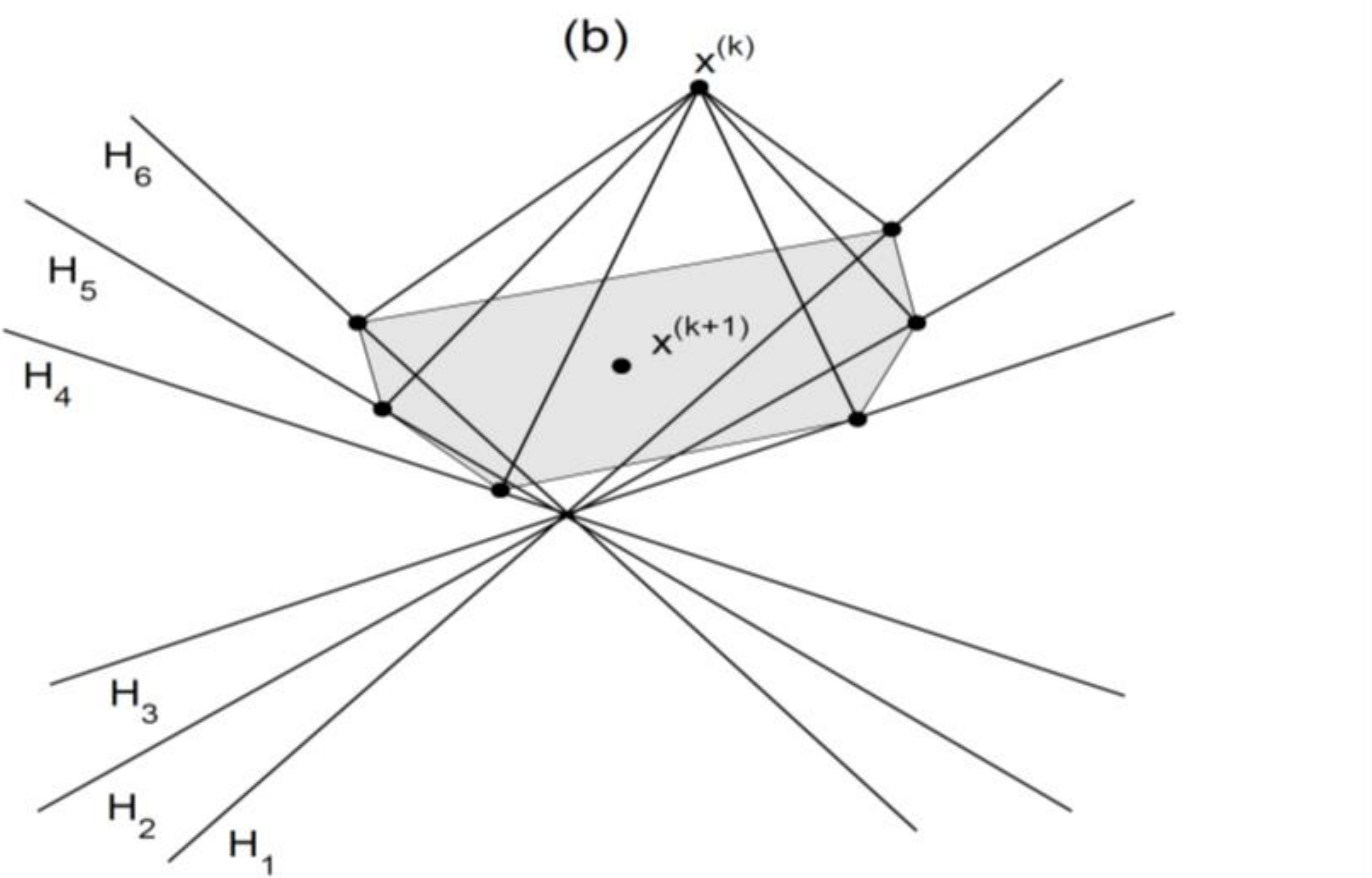

INFN-Prima pCT apparatus

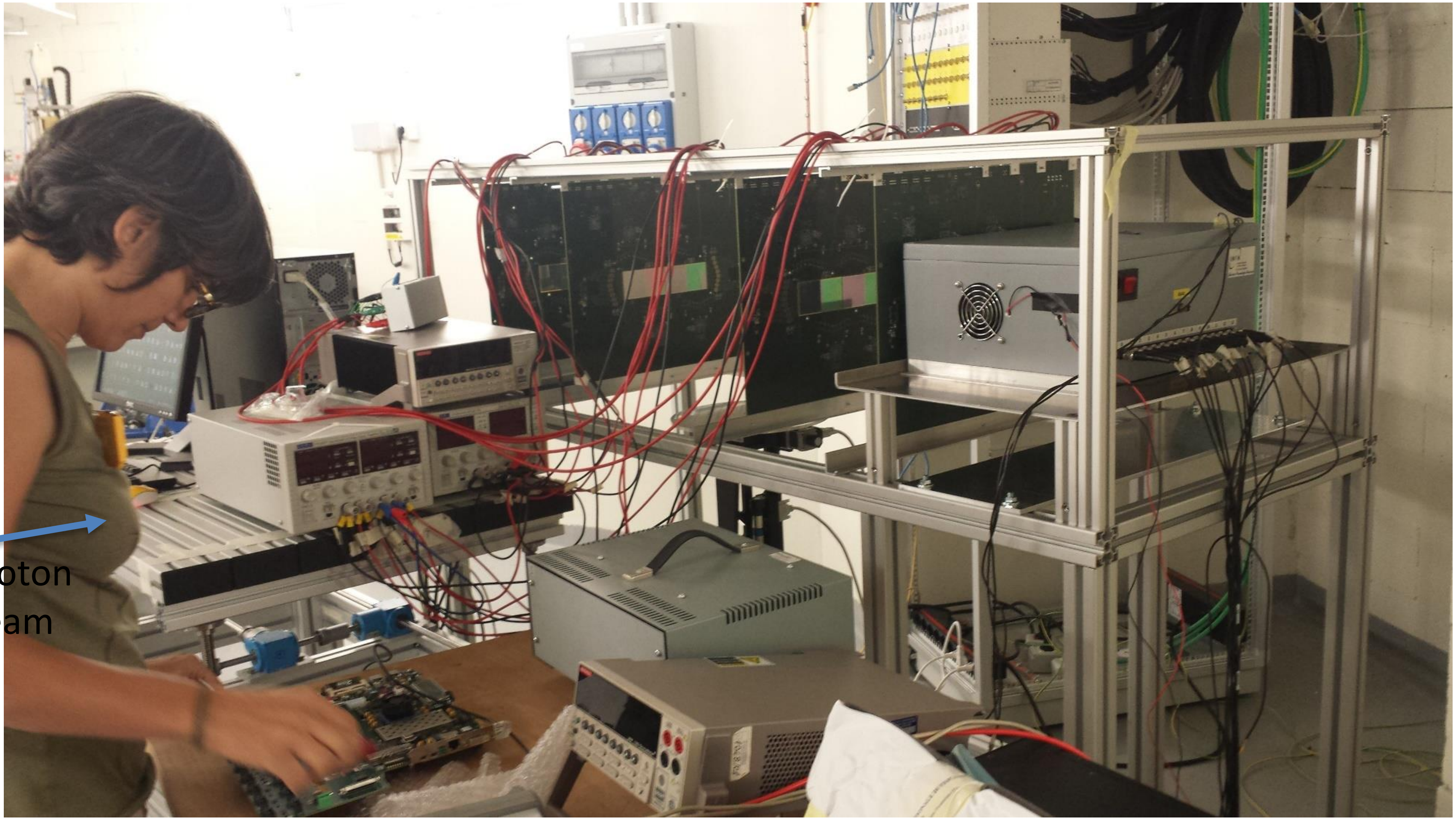

Beam test at Trento proton Therapy Center experimental beam line

Proton energy: nominal 211 MeV (198 MeV at phantom) 5x20 cm^2 field-of-view

Tracker

- 4 Tracker planes
  - 4x2 silicon microstrip p-on-n sensors (HPK + FBK production), 200μm pitch, 320μm thick
  - 6x8 front-end chips (discriminators - 32 channels each), single channel I^2C programmable thresholds → designed in collaboration with INFN-Cagliari
  - 2 levels FPGA (data reduction + event building + serial transmission)
  - 8 data + clk serial lines (1.6Gbs)
- Central DAQ board
  - ML605 Xilinx Virtex 6 development board (1GB DDR3 memory + 1Gbs Ethernet interface + I2C + RS232) → 3° level FPGA
  - FMC Interface board (serial receivers + handshake + I^2C+ spares)

Tracker plane

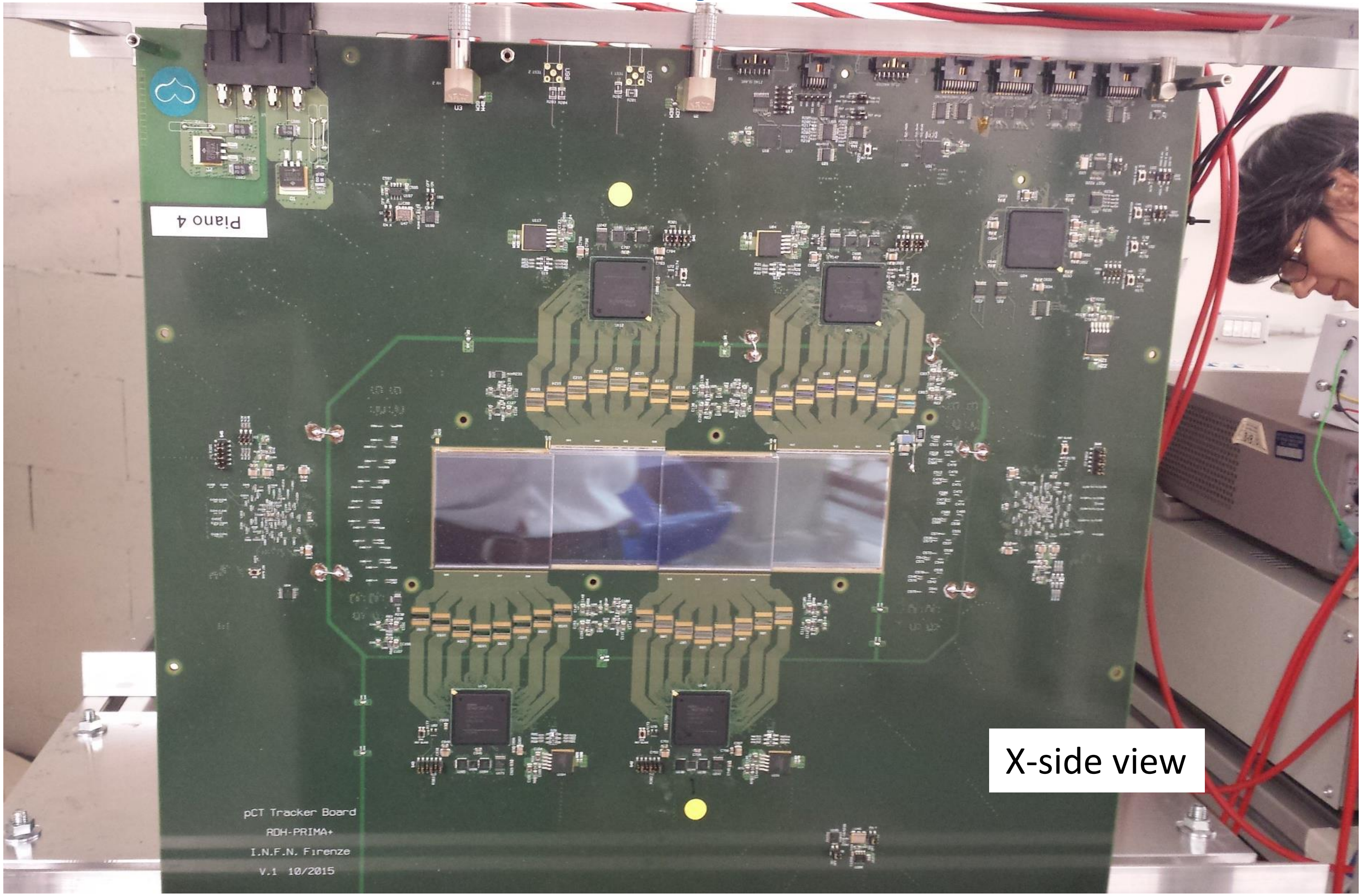

X-side view

Tracker architecture

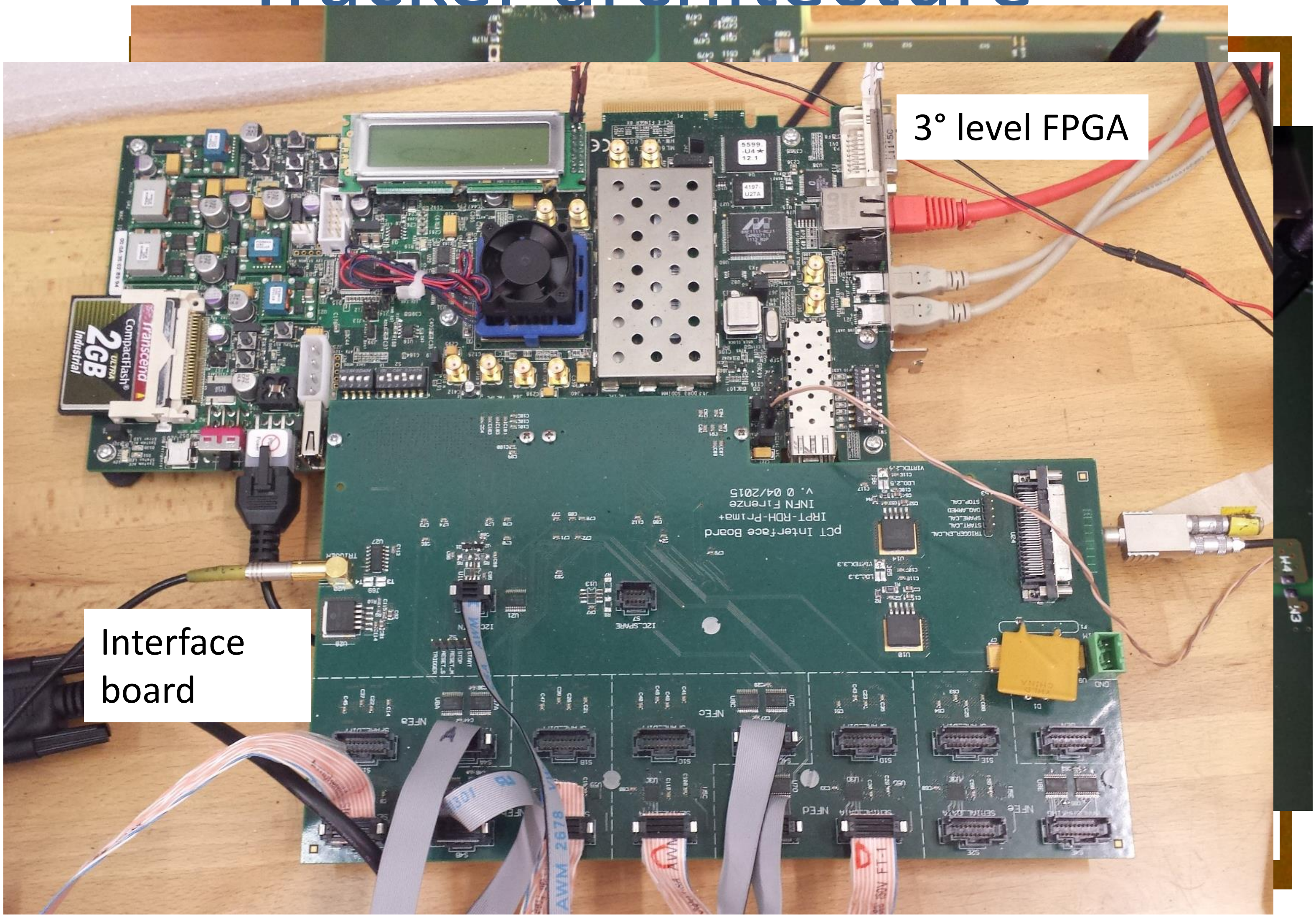

Calorimeter

- 2x7 YAG:Ce crystals
  - $3x3x10\ cm^3$
  - 70 ns scintillating light decay time
  - Hamamatsu 18x18 mm^2 photodiodes (S3204)
  - Analogue amplifier + shaper (1μs)
- NI-5751 ADC (14 bits - 5 MHz sampling)
- Main trigger generator + sync info
  - Independent crystal trigger logic
  - Neighbourhood merging (4-6 elements)
  - 7 bit event number to tracker for synchronism

Calorimeter

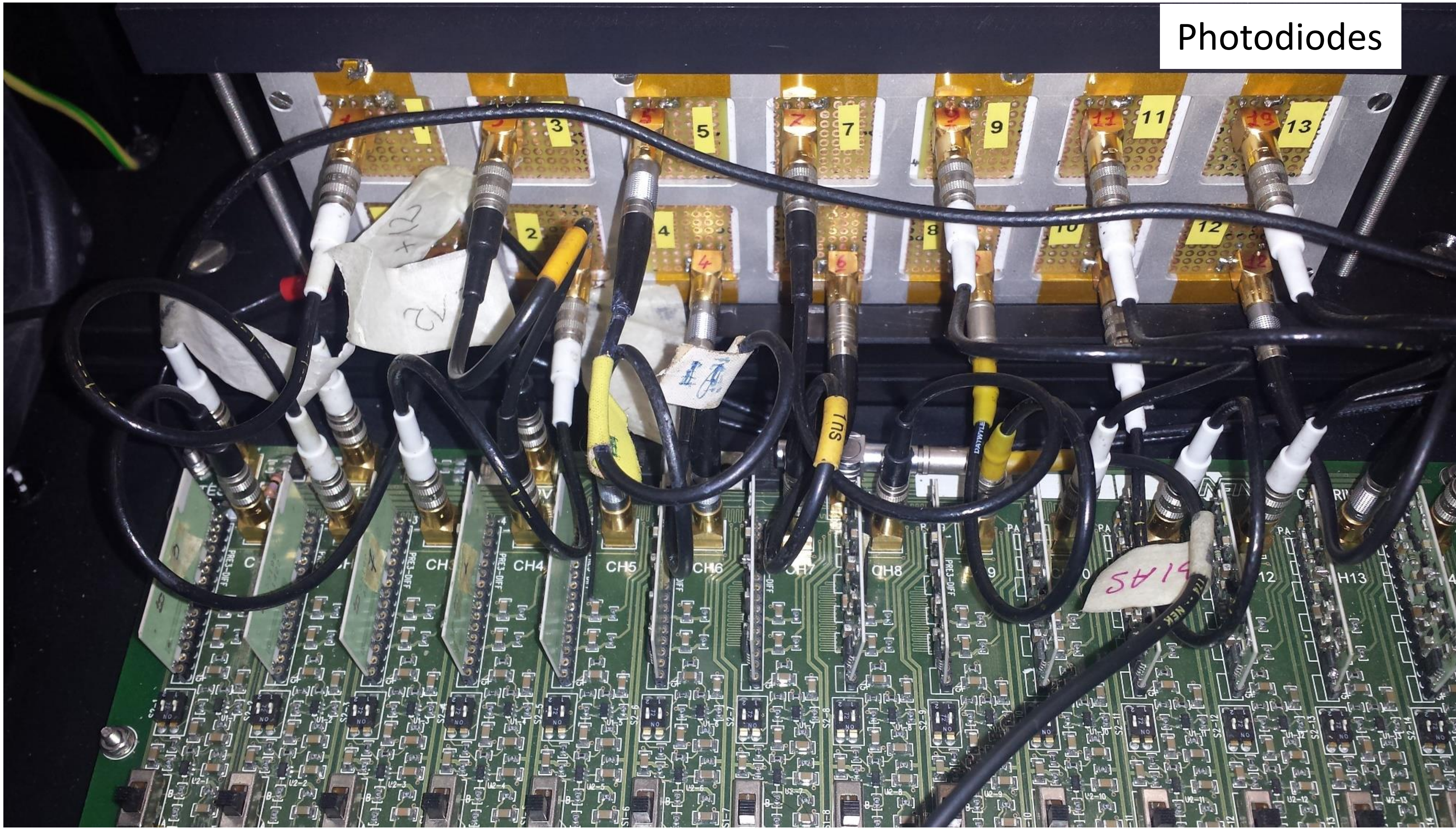

Calorimeter front-end board

Phantoms

- Two CIRS phantoms
  - Electron density calibration phantom
    - 18 cm diameter, 5 cm height: Water equivalent container + 9 plugs
  - Anthropomorphous phantom
    - Human head with titanium spine prosthesis and tungsten dental filling
- Motorized platform
  - Inserted between plane 2 and 3
  - Phi and Z movements (Physik Instrumente, linear and step motors)
  - RS232 remotely controlled – integrated into DAQ

Electron density phantom

→8 lateral plugs:

1) Liver 1.07 gcm^{-3}
2) Lung exhale 0.50 gcm^{-3}
3) Breast 0.99 gcm^{-3}
4) Bone 1.53 gcm^{-3}
5) Muscle 1.06 gcm^{-3}
6) Bone 1.16 gcm^{-3}
7) Adipose 0.96 gcm^{-3}
8) Lung inhale 0.20 gcm^{-3}

→Central plug:
Liquid water vial

→All of them embedded into a 'water equivalent' plastic material (Plastic Water LR)

Results

- Data have been collected using the experimental beam line of the Trento Proton Therapy Centre (June 2018)
- Two sets of data for tomography reconstruction
  - Electron density phantom
    - $\sim 10^8$ events in 400 angles
  - Anthropomorphic phantom
    - $\sim 1.2 \times 10^8$ events in 400 angles
- Two energy scans for calorimeter calibration
  - 6 energies $\sim 10^7$ events each (211, 193, 169, 143, 112, 83) MeV
- Two high statistics alignment run
  - 10^7 events each at 211 MeV

Electron density phantom tomography

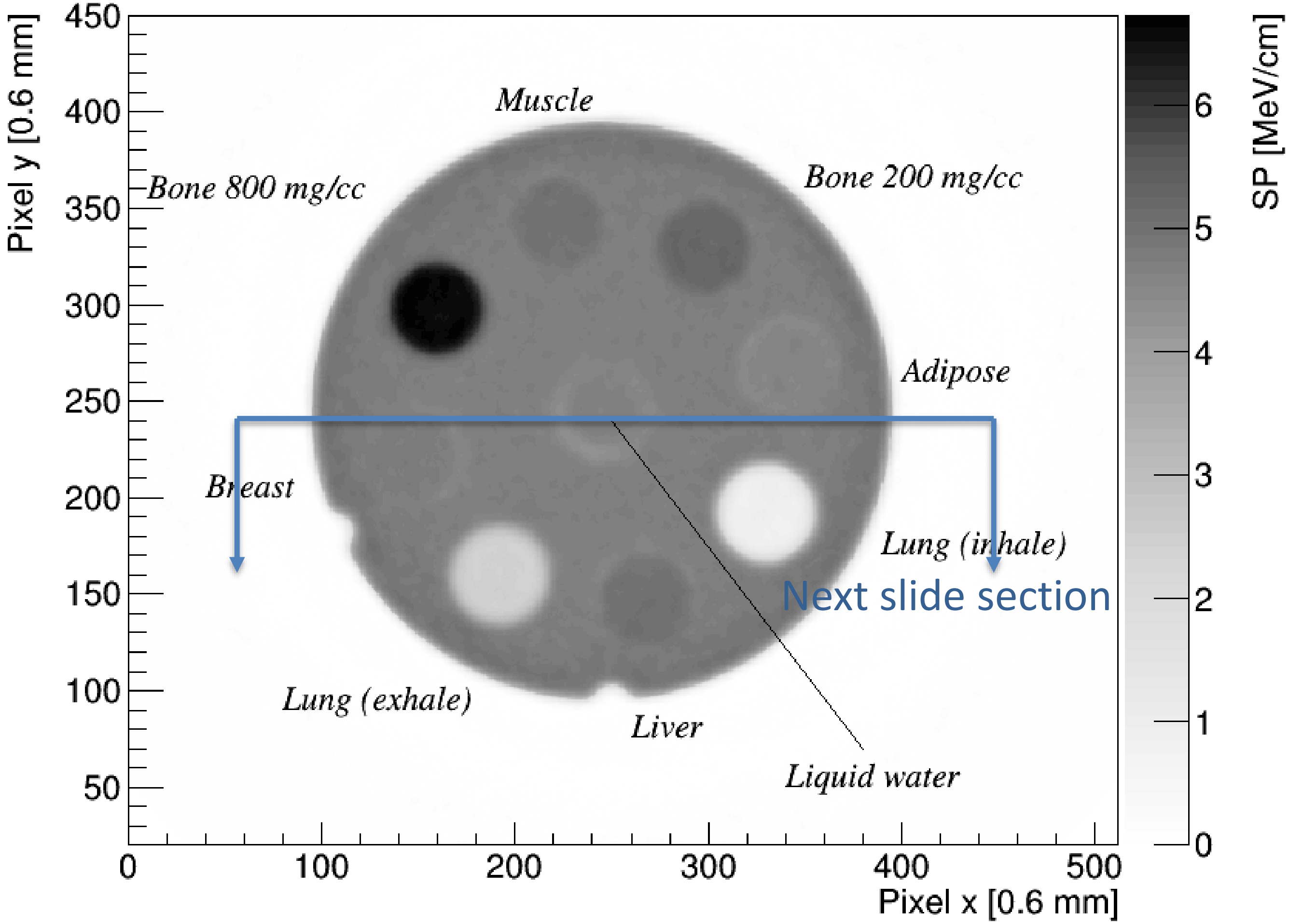

All tissue substitute inserts are visible and a quantitative analysis has been done → next slide

Radial artefacts were eliminated decreasing the tomography angular step resulting in an better quality of the image

1.6mm thick central slice of the tomography Algebraic reconstruction: 75th iteration

Electron density phantom tomography

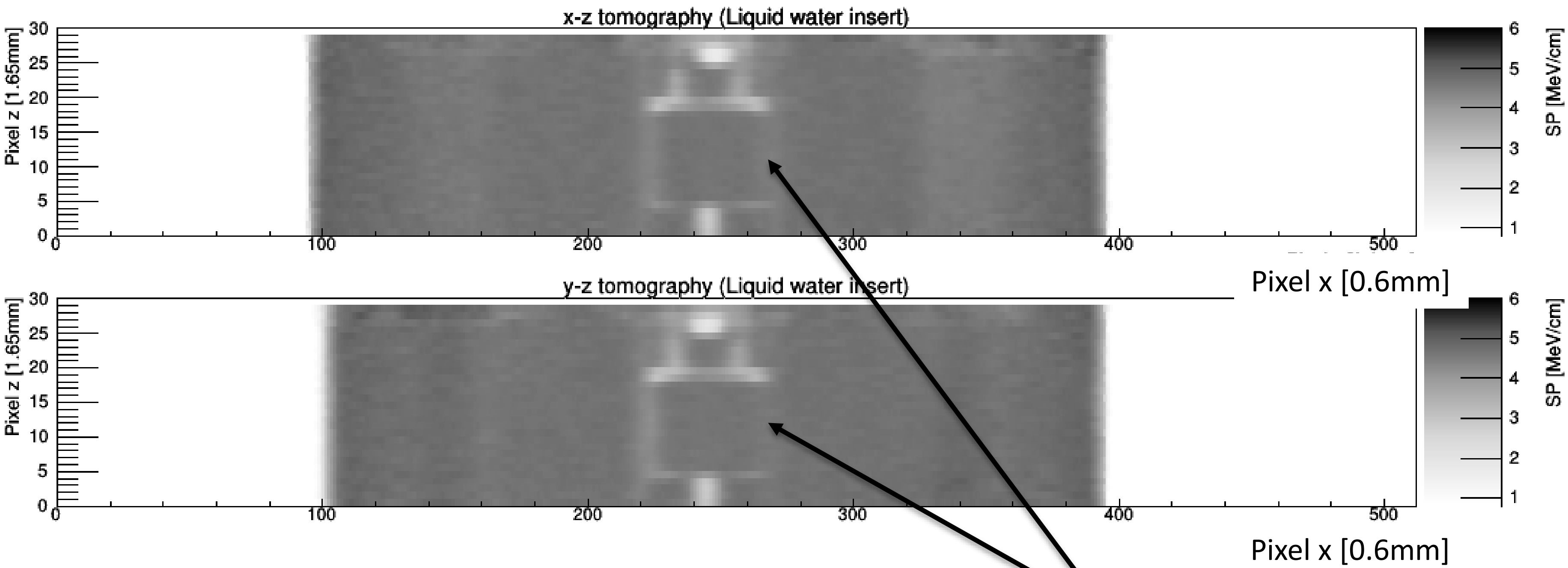

0.6mm thick vertical slice of the tomography

Distilled water vial

The distilled water vial has been used to normalize the Stopping Power values obtaining the Relative Stopping Power.

Algebraic reconstruction: 75th iteration

Electron density phantom tomography

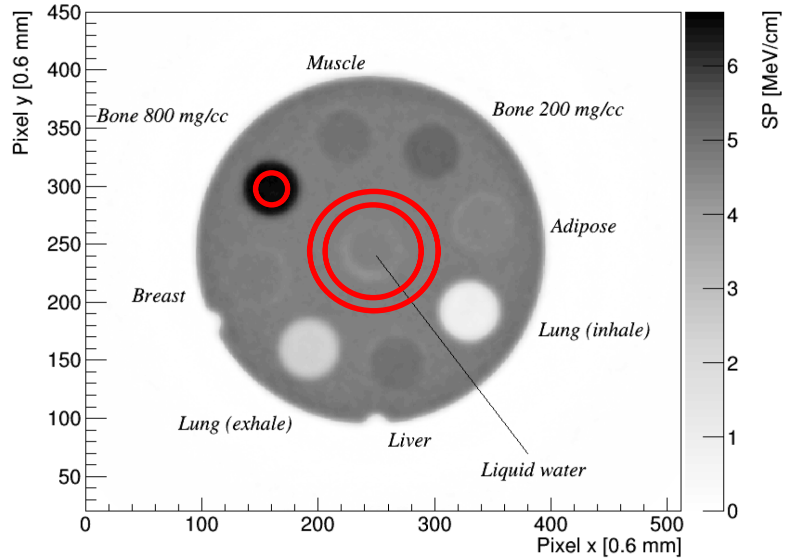

In red the fiducial regions to define the RSP values are drawn

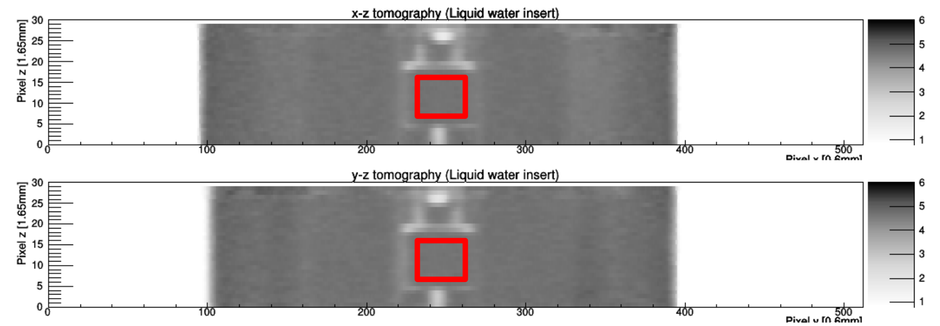

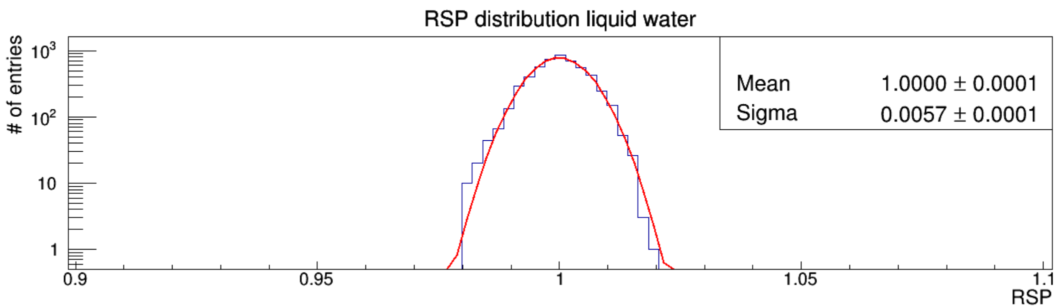

RSP of distilled water

σ=0.6%

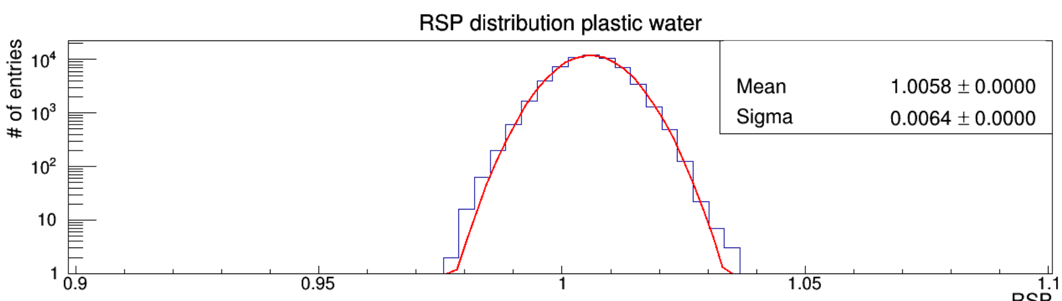

The measured RSP of the Plastic Water is 1.0058 (expected value 1.008)

σ=0.6%

Expected RSP calculation

The expected RSP have been calculated using Geant4 simulation using the G4EmStandardPhysics_option3 dataset recommended for medical Physics applications.

The tissues substitutes elemental composition and density have been inserted into Geant4 and the SP values @180MeV extracted.

E.g. for the Plastic water:
$\rho = 1.029$ g/cm^3
H = 7.91%
C = 53.62%
N = 1.74%
O = 27.21%
Mg = 9.29%
Cl = 0.23%

The Bragg additive rule has been used

→ SP (180MeV) = 4.822 [MeV/cm]

E.g. for distilled water:
$\rho = 1.000$ g/cm^3
H 11.19%
O 88.81%

Mean ionization energy I = 78 eV

→ SP (180MeV) = 4.792 [MeV/cm]

Then all expected RSPs have been corrected by the 22°C water density ρ=0.9978 g/cm^3

RSP correlation

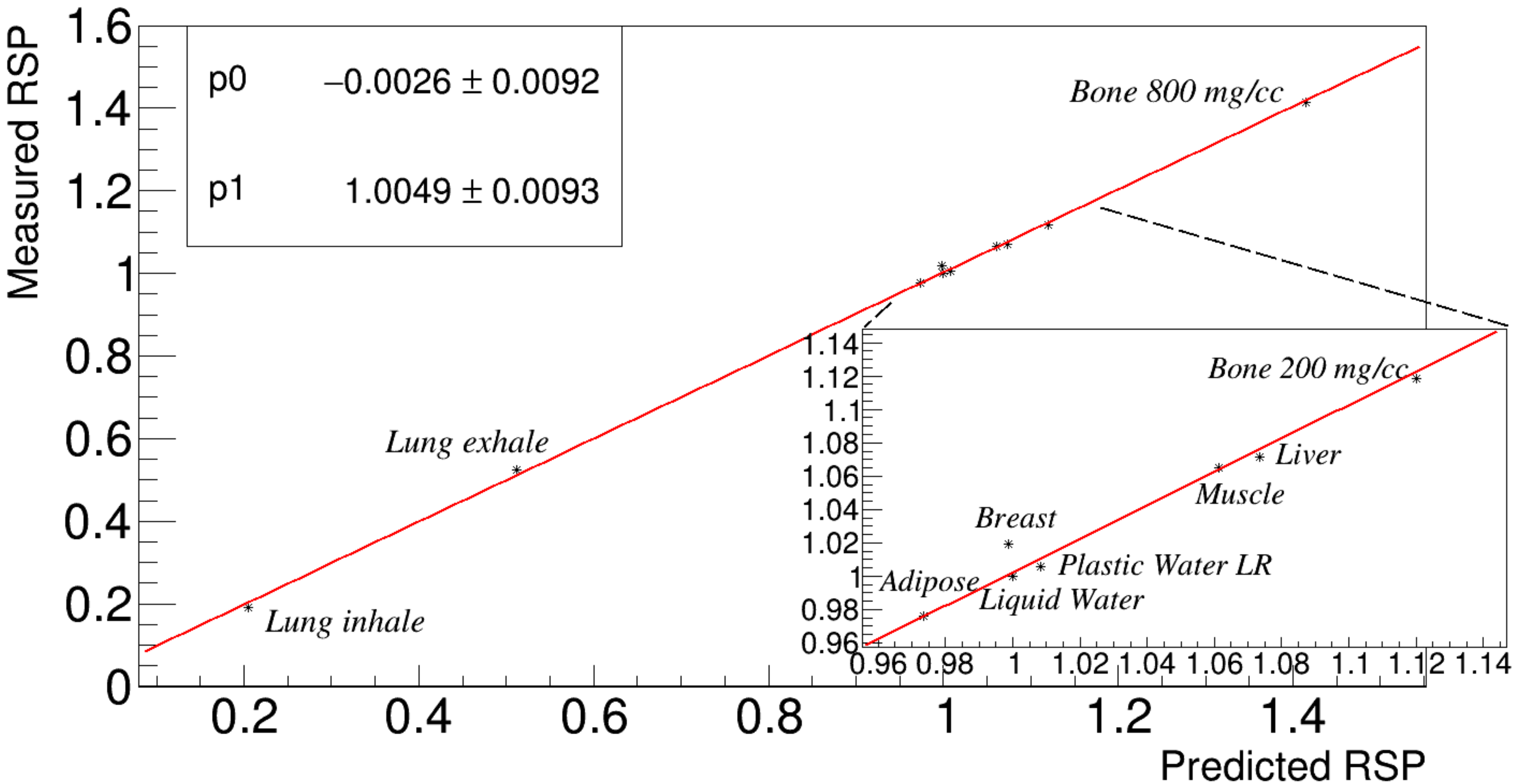

The breast substitute tissue value is still an open issue (waiting for data sheet from CIRS)

Anthropomorphous phantom tomography

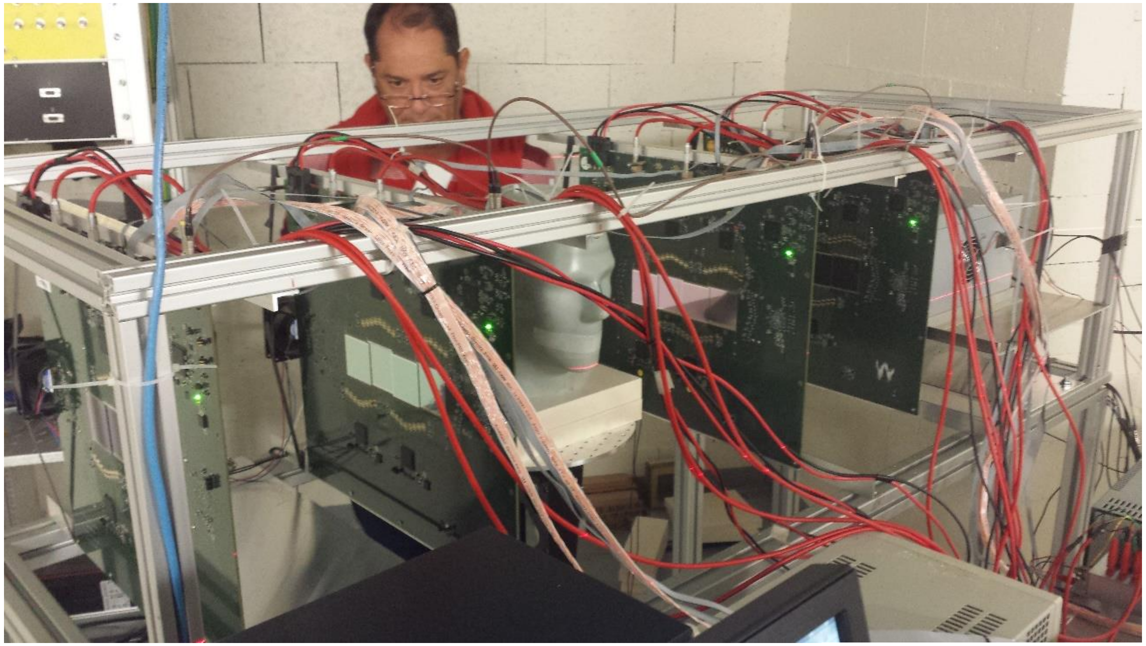

CIRS Proton Therapy dosimetry head. Mod. 731 HN

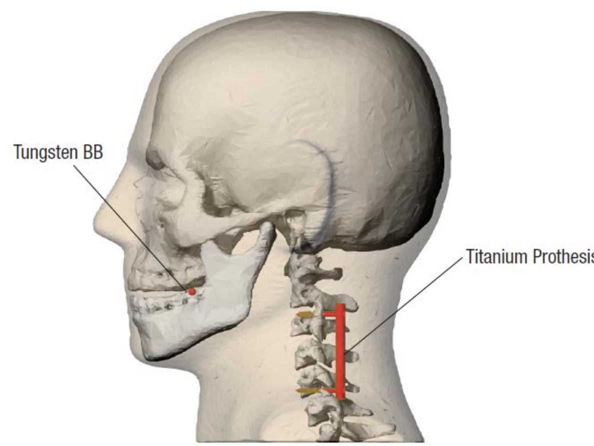

Model 731-HN Sagittal Rendering

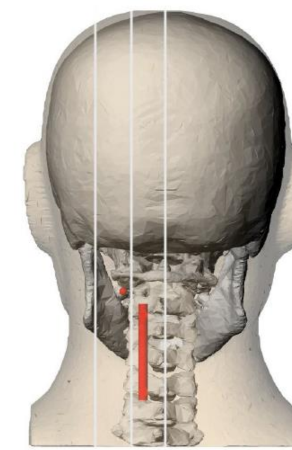
Back view of phantom with sagittal cuts

Anthropomorphous phantom

X-Rays radiographies

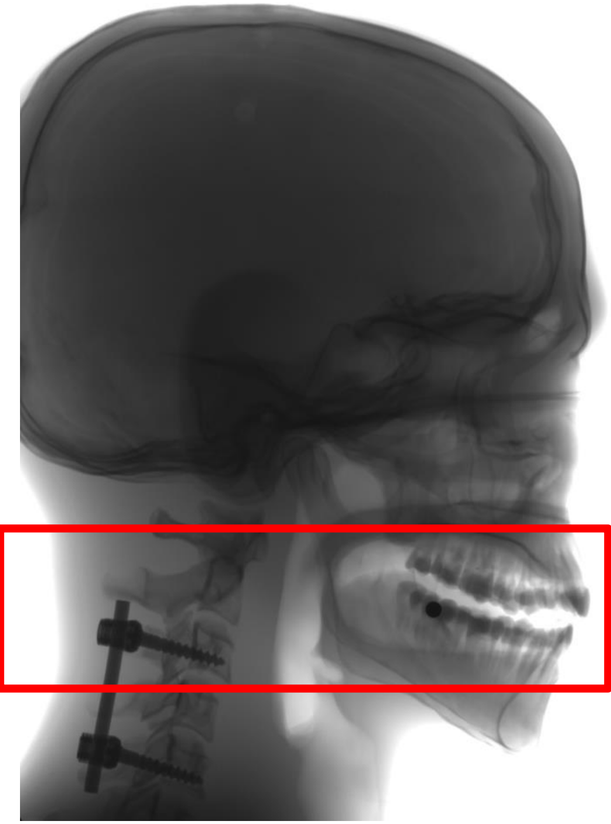

Tomography region

Dental filling in a molar
Spine prosthesis attache

Anthropomorphous phantom tomography

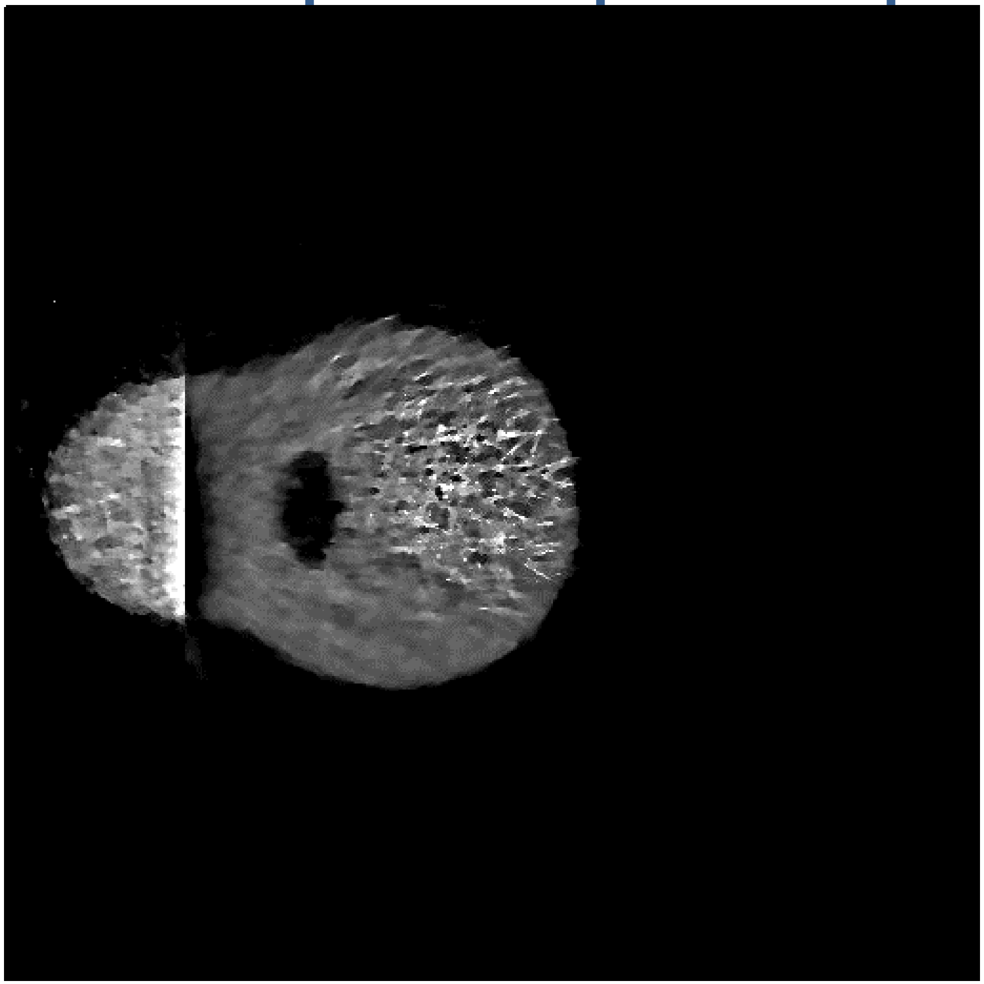

Algebraic reconstruction: 62th iteration

64 axial slices
voxels: 600x600x812μm^3 ~ 0.3mm^3

400 angles (0.9 deg. uniform spacing)
About 3.7 x 10^7 events (selected)

First and last slices have low statistics (outside field of view)
Movie starts from lower jaw ends at upper teeth (5.2 cm range)

Total estimated dose ~ 1.5mGy

Much lower contrast with respect to the X-Ray images mainly because of the physics of the interactions: important <u>Z dependence for X-Ray</u>, **<u>density dependence for protons</u>** → BUT it is what is needed for hadron therapy

Anthropomorphous phantom tomography

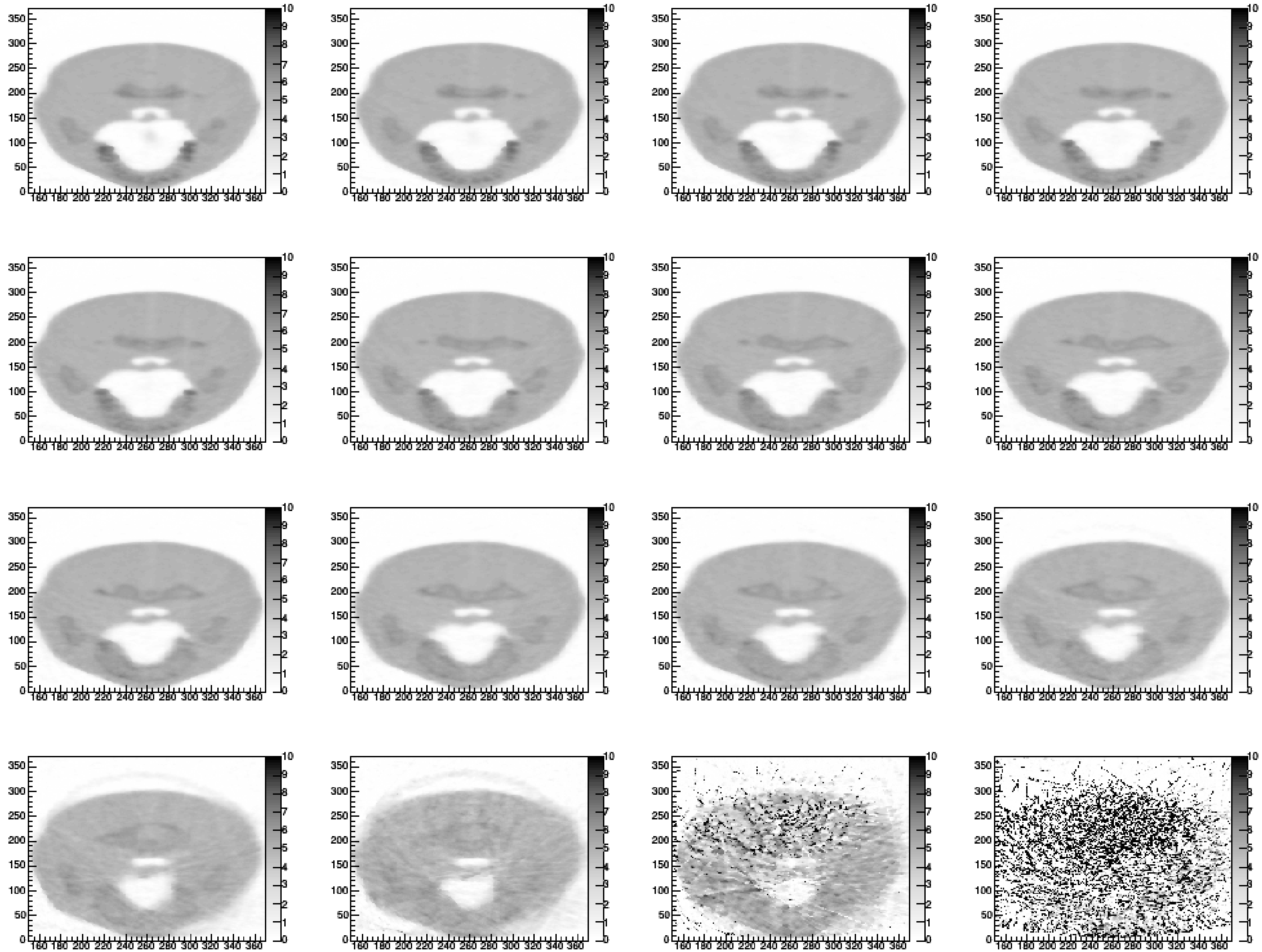

Anthropomorphous phantom tomography

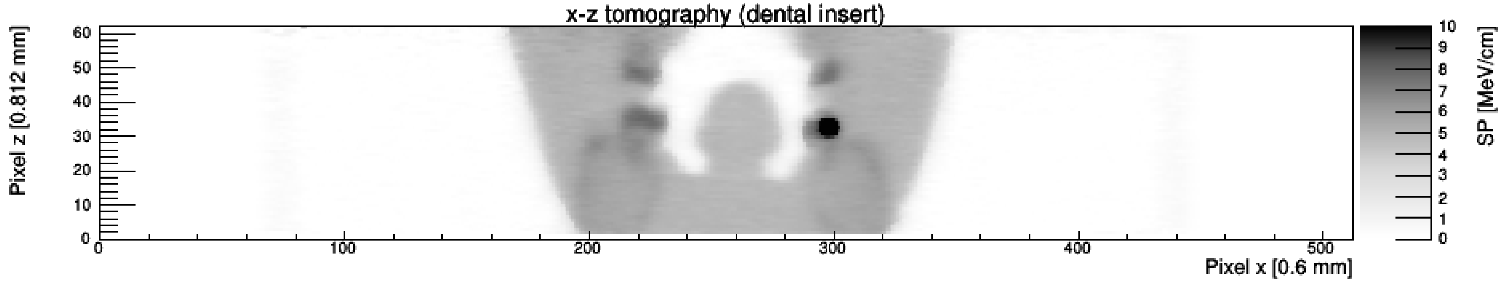

Front (coronal) view

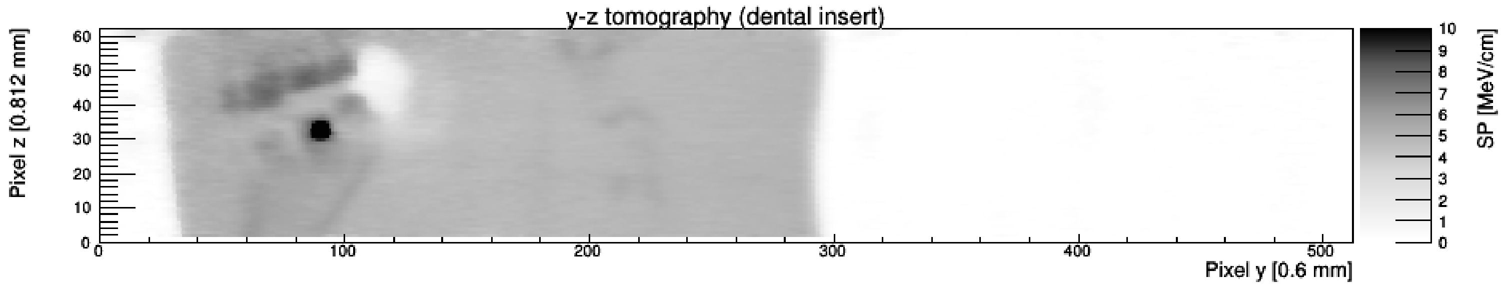

Lateral (sagittal) view

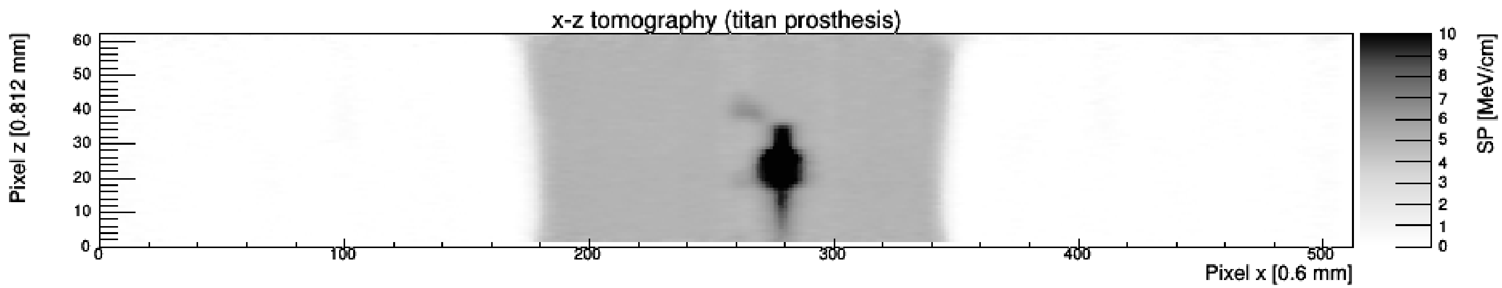

Front (coronal) view

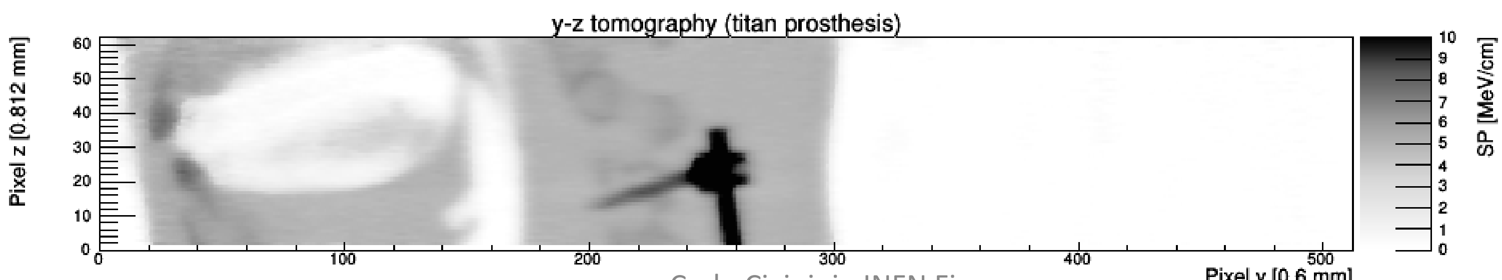

Lateral (sagittal) view

Anthropomorphous phantom tomography

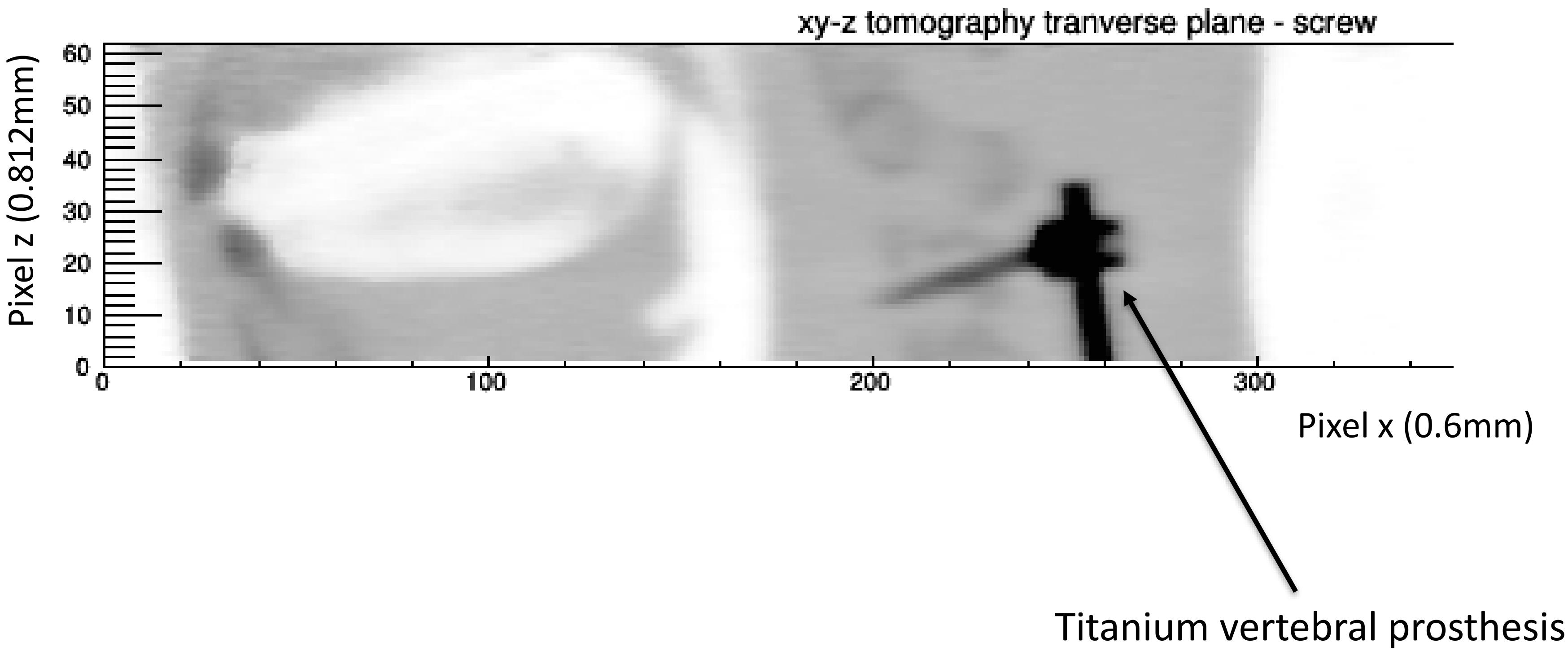

Metallic prosthesis artefacts

- Treatment plans in presence of implanted metal prosthesis are difficult to define because of xCT severe artefacts which degrade the RSP maps quality
- pCT is less sensitive to high Z materials than xCT → more accurate RSP maps close to the implants

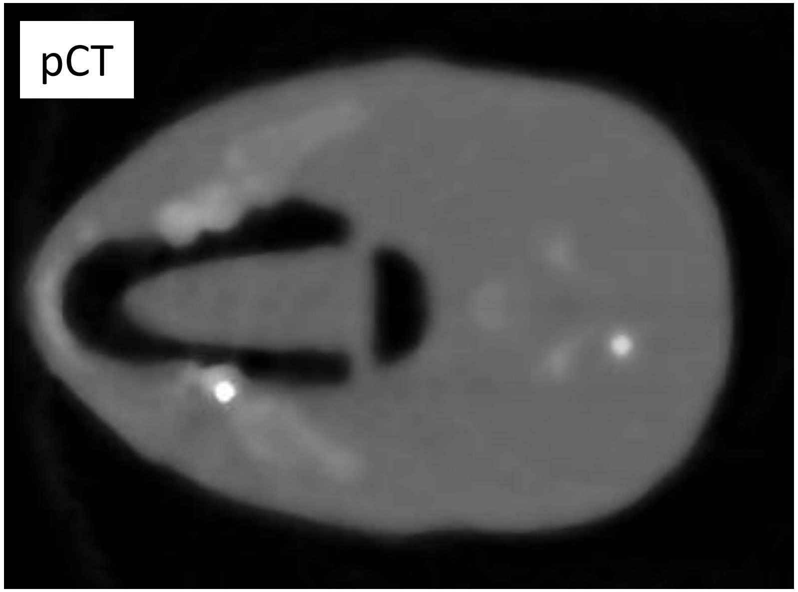

Tests are planned to quantify the influence of these structures on the treatment quality

Conclusions

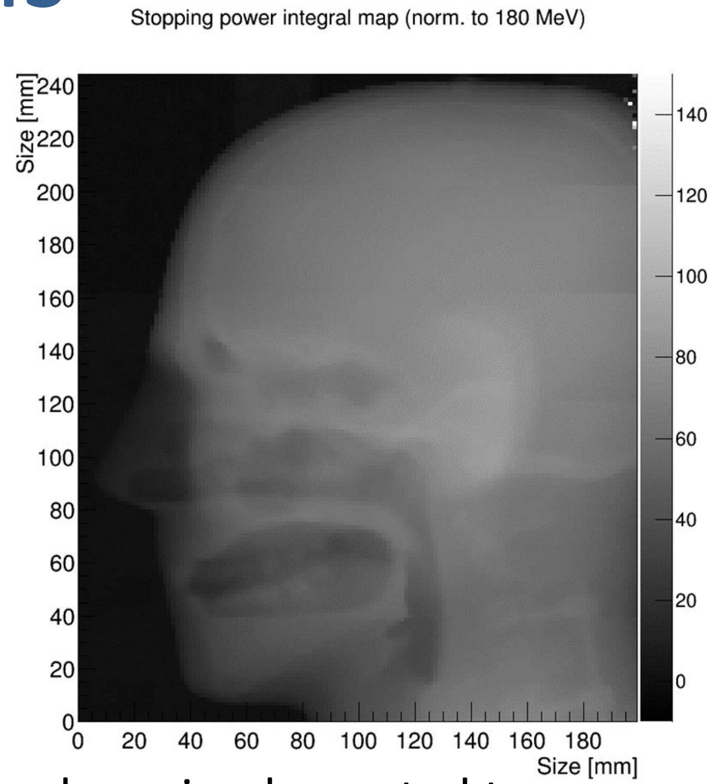

- A silicon tracker / scintillator calorimeter, 5x20 cm^2 field of view, Computed Tomography apparatus has been tested in a 211 MeV proton beam for pre-clinical studies;
- Tissue equivalent non-homogeneous phantoms have been used for tomographic data taking at the Trento proton Therapy Centre;
- Measured RSP values agree with the expected ones at level of 1%;
- Algebraic iterative reconstruction algorithms have been implemented to run on GPU;
- 3D images with 16.8M voxels with size of 600x600x812μm (~0.3 mm^3) have been reconstructed;
- Tests to define real treatment plans in presence of metallic prosthesis are foreseen.

Backup slides

proton Computed Tomography: principle

Proton Radiotherapy → first proposed by R.R. Wilson in 1946
"Radiological Use of Fast Protons", Radiology, 47:487-491 (1946)

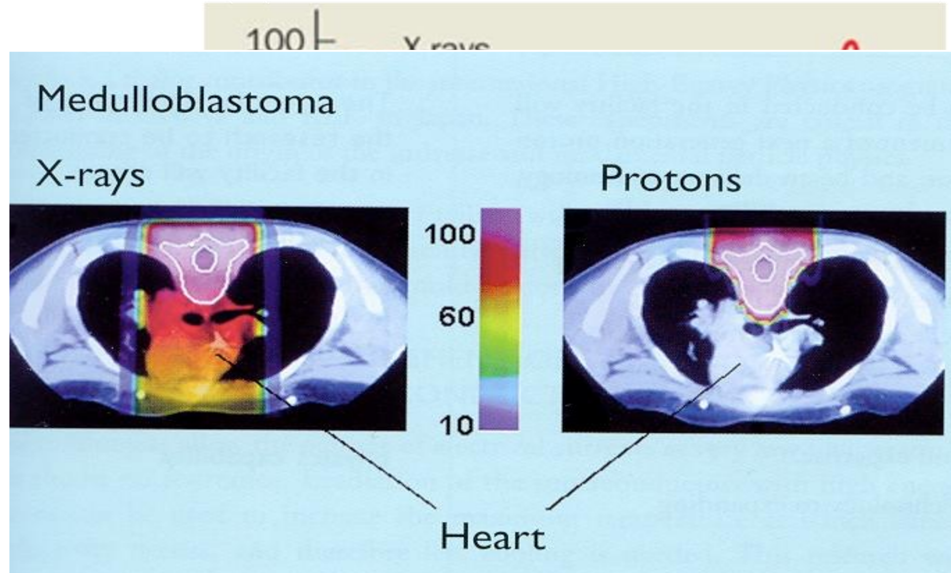

Advantage :

Highly conformational dose distribution:
i) lower dose to healthy tissues in front of tumor;
ii) healthy tissues beyond it are not damaged;

Inaccuracies: Treatment planning presently performed by X-CT → expected errors typically of a few millimeters

B. Schaffner and E. Pedroni Phys. Med. Biol. **43 (1998) 1579–1592**

pCT

- ✓ Direct measure of the 3D stopping power maps using protons
- ✓ Precision improvement when positioning and treatment are made in one go

Proton-Photon irradiation

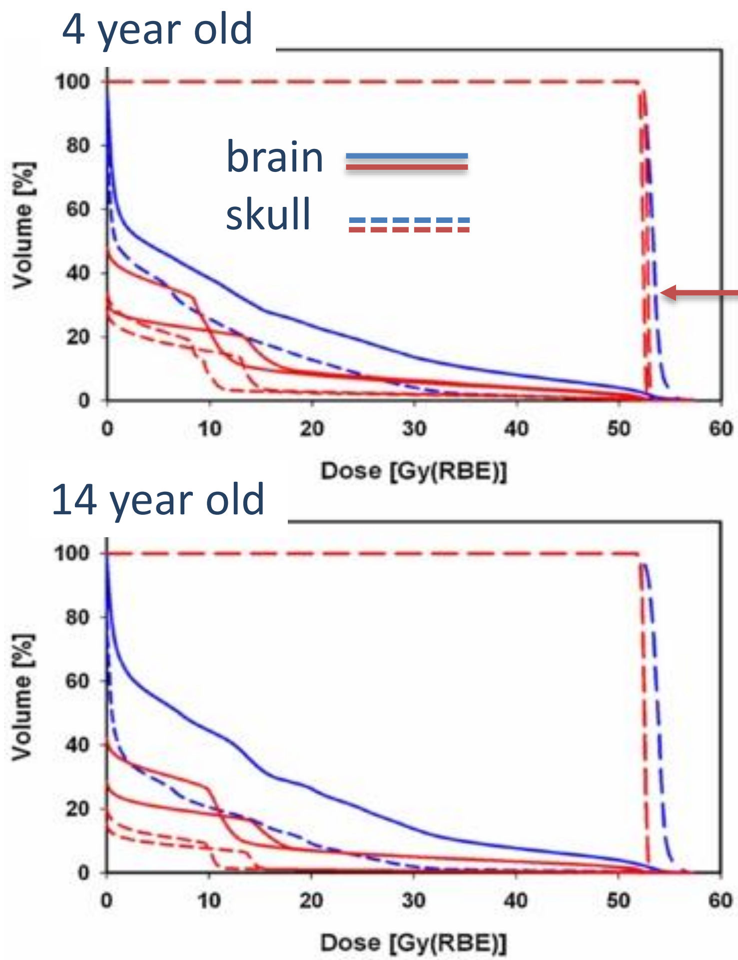

An example: optic glioma

Red: proton plan

Blue: photon IMRT plan

Target volume

Dose–volume histograms for a 4 year old (upper) and 14 year old (lower) optic glioma patient. Blue: IMRT plan; red: proton therapy plans (three and four fields). Long-dashed: target volume (not distinguishable); solid: brain (excluding target volume); short-dashed: skull.

Figure 2 from Assessment of radiation-induced second cancer risks in proton therapy and IMRT for organs inside the primary radiation field Harald Paganetti et al 2012 Phys. Med. Biol. 57 6047 doi:10.1088/0031-9155/57/19/6047

Algebraic Reconstruction Techniques

- Iterative algorithm to reconstruct tomographic images (proton stopping power maps) from a set of single proton events
- Starting point (*S(x,y,E)* stopping power):
- $-dE = S(x, y, E)dl$
- Introducing the mass stopping power S/ρ :
- $-\frac{S}{\rho}(x, y, E_0)dE = \frac{S}{\rho}(x, y, E_0)\frac{S}{\rho}(x, y, E)\rho(x, y)dl$
- E_0 being a reference energy at which the SP is calculated
- Dividing by S/ρ at energy E:
- $-\frac{\frac{S}{\rho}(x,y,E_0)}{\frac{S}{\rho}(x,y,E)}dE = S(x, y, E_0)dl$

Algebraic Reconstruction Techniques

- The left hand side doesn't depend too much on the material composition ($\leq 6*10^{-3}$) and could be replaced by the one measured for liquid water (NIST pstar tables - http://physics.nist.gov/PhysRefData/Star/Text/PSTAR.html):
- $-[\frac{S}{\rho}(H_2O)]_E^{E_0} dE = S(x, y, E_0) dl$
- Where
- $[\frac{S}{\rho}(H_2O)]_E^{E_0} \cong [\frac{S}{\rho}(x, y]_E^{E_0} = \frac{S}{\rho}(x, y, E_0) / \frac{S}{\rho}(x, y, E)$.

Algebraic Reconstruction Techniques

- Integrating along the proton path:
- $-\int_{E_{in}}^{E_{out}} [\frac{S}{\rho}(H_2O)]_E^{E_0} dE = \int_{path} S(x,y,E_0) dl$

D. Wang, Med.Phys. **37** (8) (2010) 4138-4145.

- E_{in} is given by the accelerator, E_{out} by the calorimeter and the '*path*' by the tracker (Most Likely Path)
- Subdividing the object into a set of pixels, for the *i*th proton:

$$p_i \equiv -\int_{E_{in}}^{E_{out}} [\frac{S}{\rho}(H_2O)]_E^{E_0} dE = \sum_{j=1}^{N} w_{ij} S_j(E_0) \qquad i = 1, \dots, M$$

- Where w_{ij} is the path length of proton *i* inside the pixel *j*

Motorized platform

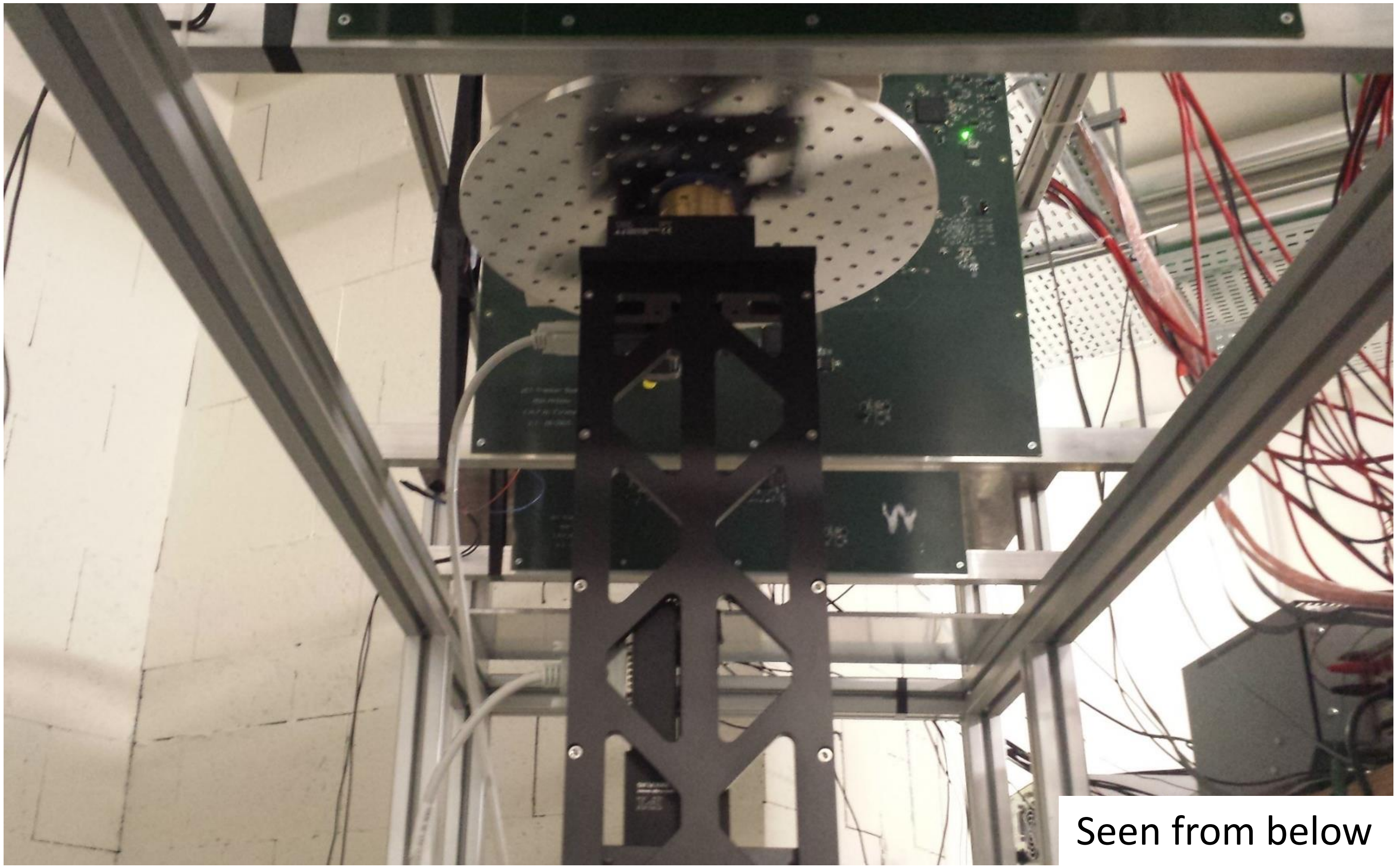

Seen from below

Off-center axis (5 cm) to allow tomographies of large objects

Large area system: radiography

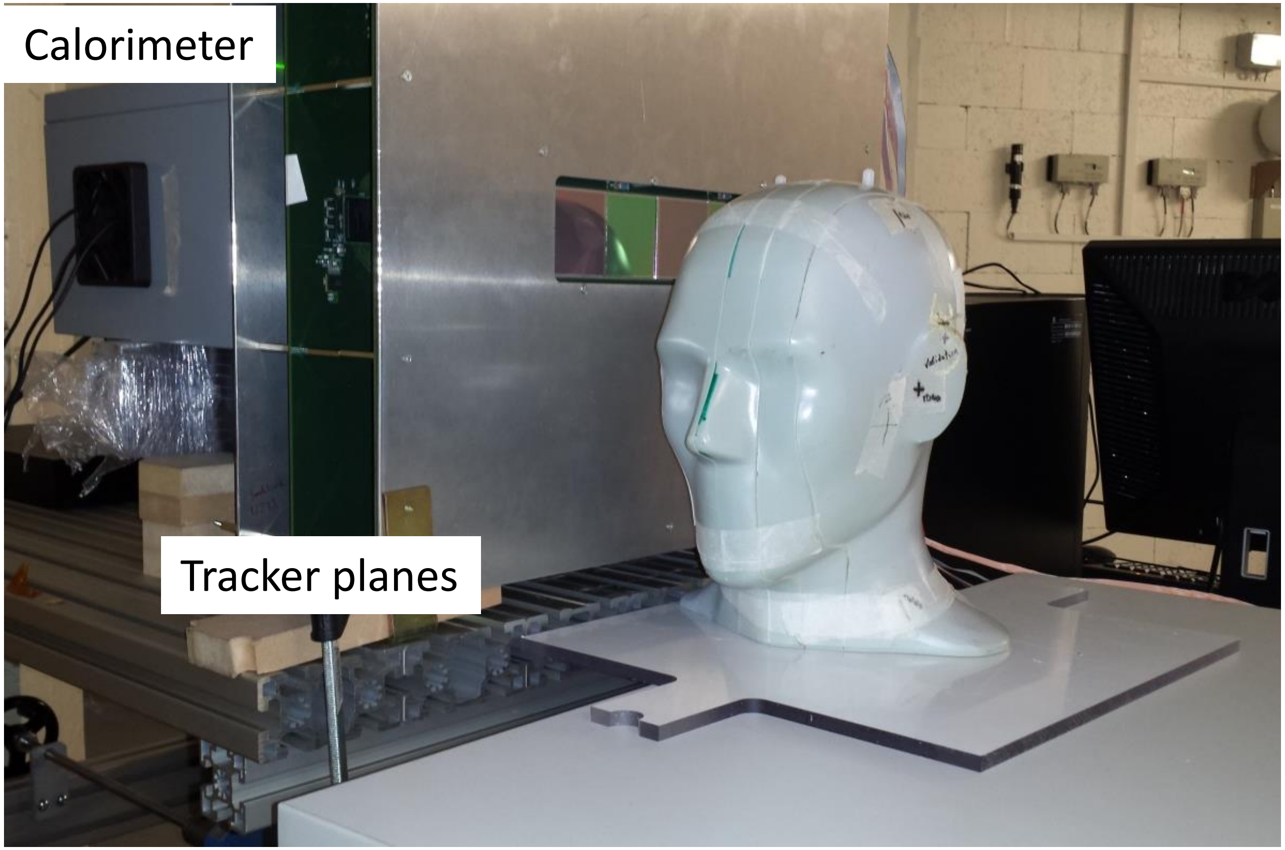

At 'Centro Protonterapia' Trento, Italy - October 2016

Intermediate step to full Tomography

Two tracker planes and Calorimeter

CIRS Antropomorfic phantom

Two tracker planes to extrapolate the exiting proton trajectory to the calorimeter for better energy resolution and back to the head mean transverse plane for image reconstruction.
Beam energy to the phantom : 180 MeV. About 10^7 protons per slice → 90 μGy

Large area system: radiography

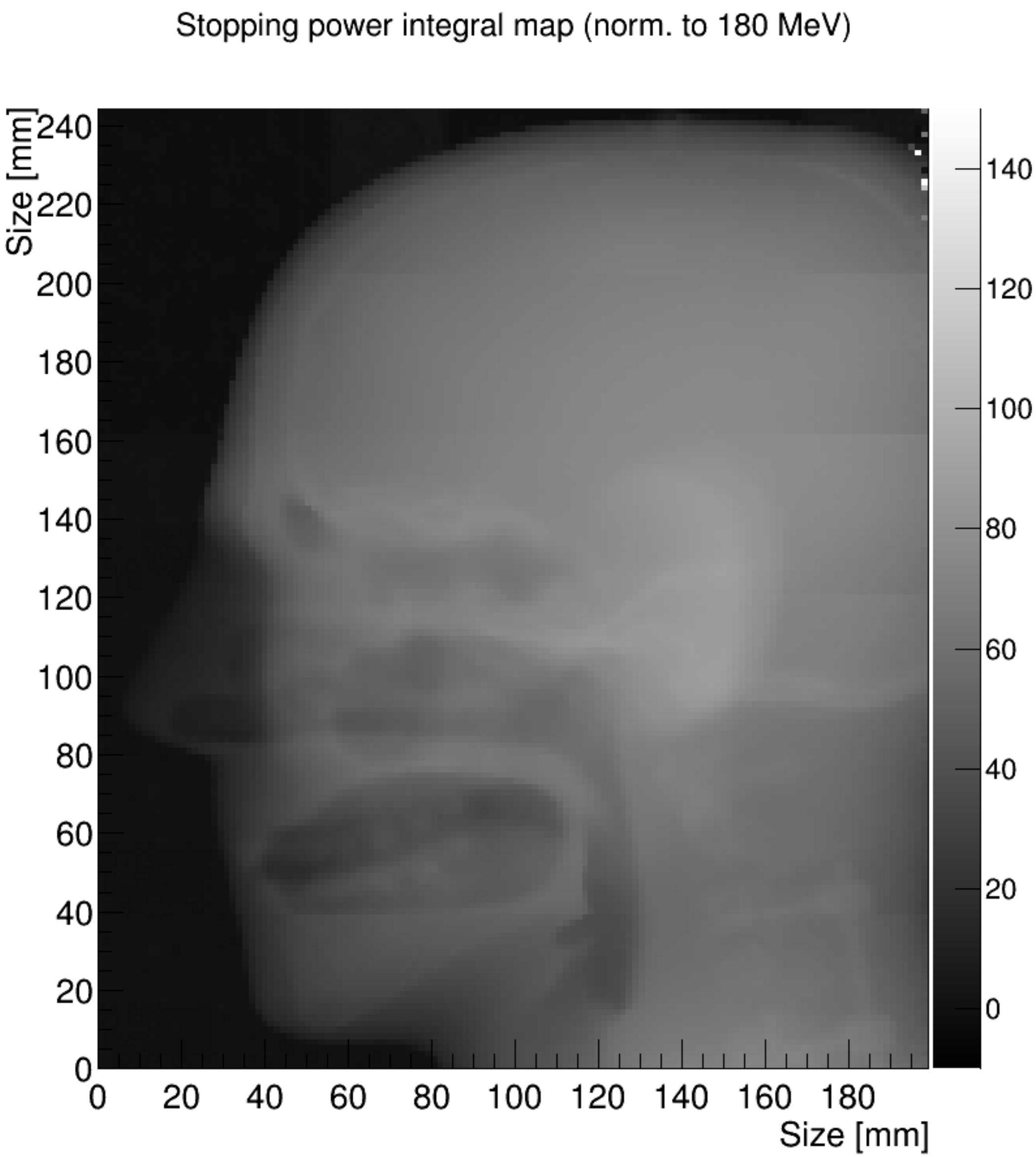

Stopping power integral map normalized to 180 MeV (same quantity used for Tomographic Reconstruction):

Pixel size 1.5mm
Beam energy 180 MeV
No MLP

Many thanks to TIFPA, IBA and 'Centro Protonterapia', Trento

Large area system: radiography

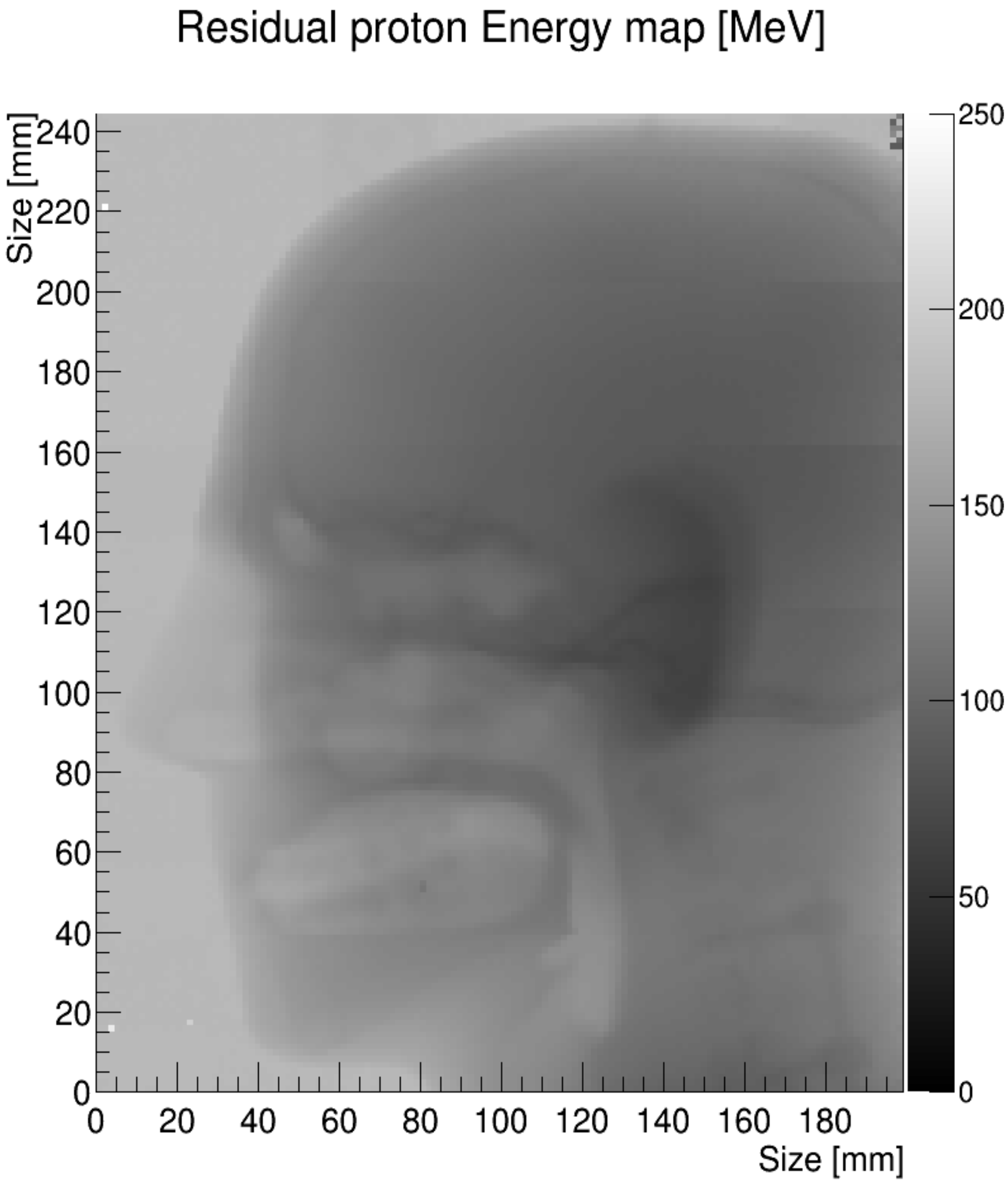

Residual energy map:

Pixel size 1.5mm
Beam energy 181 MeV
Dose 90 μGy